FACTURE KINETICS OF CERAMIC MATERIALS IN CONTROLLED CRACK GROWTH TEST

S.P. KOVALEV, V.M. CHUSHKO and V.G. BOROVIK
Institute for Problems of Strength
Academy of Sciences of the Ukraine, Kiev 252014, Ukraine

ABSTRACT

A method of fracture testing with controlled crack growth in ceramics is used for studying crack kinetics behavior under the given loading history. A computer-aided real-time data acquisition system enhances the informativity of a simple single specimen bend test in quantification of the crack growth parameters. Controlled fracture data are shown for alumina and for two grades of yttria-stabilized zirconia, all suggesting microstructure dependent fracture properties. Observed ambiguities in the crack growth diagrams for controlled testing are discussed to demonstrate the importance of the consideration of a crack growth history for the correct description of inequilibrium fracture behavior.

KEYWORDS

Fracture kinetics, R-curve, slow crack growth, alumina, zirconia

INTRODUCTION

Nonlinear fracture effects caused by the crack interaction with ceramic microstructure give rise to the obvious crack growth parameters dependence on the loading history. As a result in the lifetime prediction for ceramic structural elements the problems of undesired errors arise because of the uncertainty in the slow crack growth parameters. For the purpose of quantification and appropriate simulation of possible ambiguities in slow crack growth behavior the methodology of controlled fracture testing under predetermined loading history seems to be promising for better understanding of fracture kinetics.

The present paper addresses the question of controlled fracture testing with the emphasis on the crack kinetics monitoring, which is based on the improvement of displacement-controlled fracture testing in a stiff loading device. Some characteristic fracture kinetics data for alumina and tetragonal zirconia polycrystals are presented. These materials are expected to exhibit the microstructure dependent fracture properties, namely, the microcrack-induced rising crack growth resistance resulting from the thermal expansion anisotropy for the former, and the transformation toughening for the latter.

EXPERIMENTAL PROCEDURE

Standard single-edge notch bend (SENB) test geometry has the monotonously rising K-calibration, which prevents to control the fracture process. The best way to the effective controlled crack growth test is to utilize the test geometries having descending part of the K-calibration curve (Munz, 1983; Freiman, 1983). Pabst (1975) was probably among the first who proposed the employment of 'stiff loading cell' for the SENB test geometry resulting in stable fracture of the specimen. Moreover, a stable crack extension under constant displacement rate is believed to give the possibility of indirect measurement of the crack velocity, thereby, receiving the V-K diagram (Kleinlein and Hübner, 1977; Fields et al, 1983; Steinbrech et al, 1983, 1984; Wilde et al, 1985). Concerning the publications mentioned, the following main problems may be noted. The crack length region for stability seems to be defined empirically, leading to the test results dependence on the testing machine rigidity, displacement rate, and on the type of starting notch (straight-through or chevron). The indirect determination of the crack velocity using the constant cross-head displacement rate is very approximate, thus, giving only an average estimate of a real velocity, and also being hardly dependent on the rigidity of the testing machine.

Substantial improvement of the fracture data acquired during controlled fracture testing may be achieved by the implementation of computer-aided data acquisition and processing (Hennicke et al, 1984; Jung et al, 1988). However, the main advantage of the computer data acquisition consists in the real-time monitoring of the crack growth. The application of controlled fracture testing together with the computer-aided real-time data acquisition could enhance the informativity of the single specimen test for ceramics and will help to avoid such traditional shortcomings of strength and fracture testing, as data scatter resulting from differences in specimens, starting notches, or testing conditions.

The schematic showing the testing arrangement is given in Fig. 1 (Borovik et al, 1990). To ensure the controlled fracture a special parallel elastic element (PEL) is used, which bears the external load P_c simultaneously with the test specimen (Borovik, 1985). In the fracture test with PEL the simple three point SENB geometry is used with a thin diamond-saw cut as a starting notch. External loading is applied via the proper choice of the cross-head displacement function $U_c(t)$ resulting from the manual control on the appropriate hydraulic testing machine. The values of the specimen load P_s and deflection u_s are monitored by the computer in real-time option under the supervision of a program, which manages data storage and post-processing. The real-time load-displacement record represents the raw data points for subsequent calculation of the fracture kinetics characteristics. Taking into account all compliance components of the loading scheme for the test specimen in Fig. 1, it is possible to derive the K-calibration of the SENB test in PEL-unit as follows:

$$K\,(t, A/W) = \frac{L\,U_c(t)}{W\,B\,W^{1/2}}\;\frac{C_{pel}\,Y(A/W)}{C_{tm}\,(C_{pel} + C_{sb}) + C_{pel}\,C_{sb}}, \qquad (1)$$

where Y(A/W) is the calibration function of conventional three-point SENB test (Srawley, 1976), L, B, and W are the specimen dimensions, A is the crack depth, C_{tm} is the testing machine compliance, C_{pel} is the PEL-unit

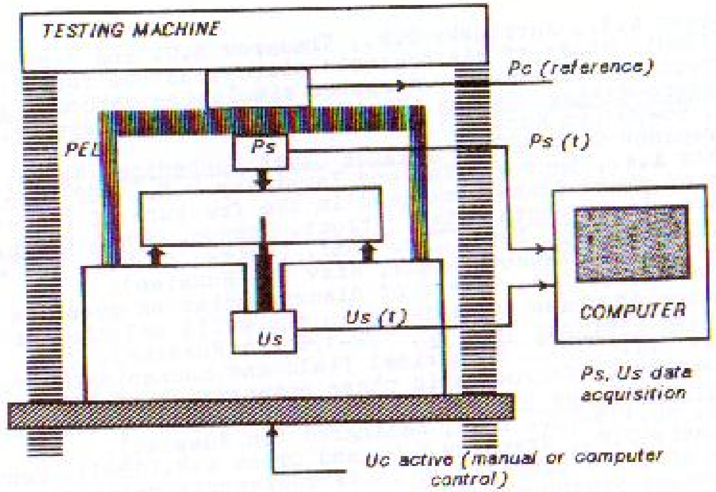

Fig. 1. Schematic of controlled fracture test apparatus for 3-point SENB specimen: PEL - parallel elastic element.

compliance, C_{sb} is the total compliance in the specimen branch contained inside the PEL-unit. As shown in Fig. 2, calibration curve (1) has a convex shape with rising and descending parts (in contrast to the monotonically rising Y-calibration). Eq. (1) is derived on the basis of linear elastic fracture mechanics, therefore, the limits of crack stability and instability are defined for a linearly elastic material. It follows from the consideration of Eq. (1), that the value of C_{tm} have a minor influence on the position of the maximum of the calibration vs crack length curve, and that the crack length for the stability of fracture may depend only on the compliance in the specimen branch C_{sb}. The specimens having starting notches close to the position of the maximum in the K-calibration should exhibit fully stable crack growth. Thus, the explicit introduction of the testing system rigidity in the K-calibration (1) allows to relate strictly the actual input and output of the fracture test, i.e., the time dependence of the stress intensity history on the cross-head displacement.

Calibration (1) may be directly employed in the stress intensity calculation for the predetermined $U_c(t)$, but it is more accurate to use conventional calibration Y with respective measurements of Ps and us. In linear elastic SENB test the current crack length $x_i = A_i/W$ may be calculated from the compliance. Usually in the compliance calculations of crack length several full or partial unloadings are used during the crack growth to define the magnitude of compliance change. By idealization of the load-displacement diagram it is possible to simplify the calculation having only two reference crack lengths, the starting, and the final. The idealization of the load-displacement diagram is based on the linearization of the loading and unloading extents of record where no crack growth is assumed. The relevance of the idealization and crack determination via compliance were estimated for each specimen by

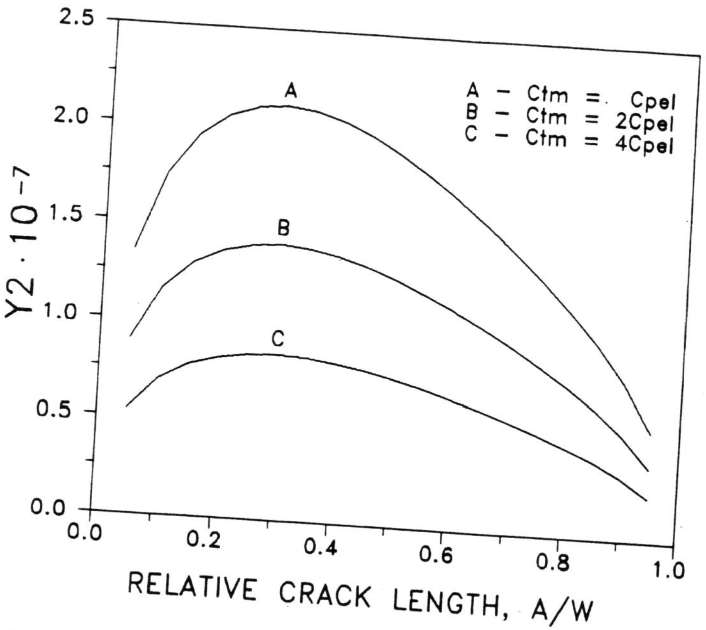

Fig. 2. The influence of testing machine compliance on the crack stability.

comparison of the calculated and visually measured initial and final crack lengths. Since the crack velocity in SENB test is not constant, it is not easy to measure actual crack length for comparison with the compliance calculations. But the final crack length is easy to measure either on the specimen side or on its fracture surface. For all the materials studied the final crack length measured by the optical microscope with resolution of 0.01 W was always closer to linear calculation.

RESULTS AND DISCUSSION

Alumina and zirconia ceramics were investigated. The alumina ceramics of AOT-grade is a MgO-doped high-purity partially translucent ceramics of relatively coarse grain-size. To investigate possible transformation toughening effects on crack kinetics two grades of 2 mol.% yttria-stabilized zirconia were tested, which may be related to the class of tetragonal zirconia polycrystals. The TZP2Y-grade has the duplex microstructure typical of the materials containing the mixture of tetragonal and cubic phases, where the major fine-grained fraction (< 1 um) is assumed to be tetragonal with imbedded coarse inclusions (5-10 um) suggested to be cubic. Another composition of zirconia ceramics (TZP2Y5A) contains additionally 5 mol.% of alumina. Mean grain size of zirconia matrix was estimated as 1 um, and that of the intergranular alumina inclusions as 2-5 um.

Alumina ceramics is expected to exhibit microstructure dependent fracture characteristics due to susceptibility to microcracking. In fact, strong ambiguities are obvious in the V-K diagram (Fig. 3). Initially the crack

starts to move with low acceleration, which results in the gradual slope of respective extent of the V-K diagram. This extent appears to reflect the behavior observed in a conventional R-curve test. Crack retardation occurs under decreasing stress intensity with a more steep slope of the V-K diagram. If additional crack extension is induced by further increment of the cross-head displacement, the acceleration branch follows the former slope, while the retardation is shifted to the higher stress intensities with an equivalent increase in the crack growth exponent (see the data for AOT-21 specimen). The comparison of data in Fig. 3 shows that the crack growth exponent for the crack retardation is proportional to the preceding crack extension, and, therefore, is dependent on the loading history. The observed dependence is similar to the reported "memory" effect (Knehans and Steinbrech, 1982), that was explained by microcracking related phenomena during the growth of a macrocrack.

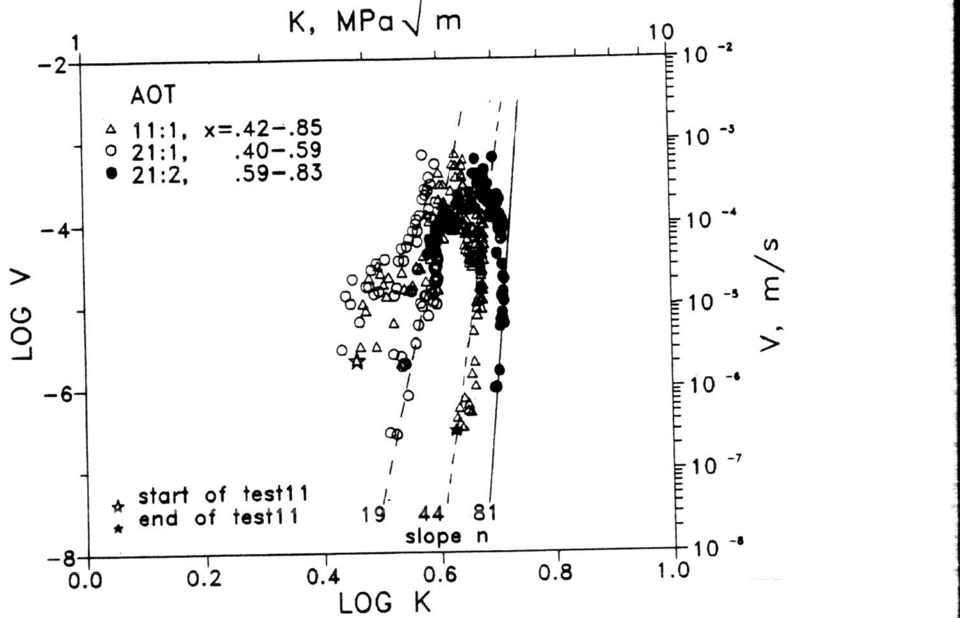

Fig. 3. Crack velocity vs stress intensity diagram for AOT-alumina showing an ambiguity both in one-run test (11), and in two-run test (21) between successive runs.

Zirconia ceramics were tested under a single or several successive crack runs on each specimen. TZP2Y as well as TZP2Y5A showed similar fracture kinetics features (Figs 4 and 5), namely, the slow crack growth diagram reveals the plateau-like middle extent. Since such behavior is hardly dependent on the loading history, it is useful to consider the test in detail. The crack starts from the notch having a relatively high stress intensity and moves with acceleration to the maximal velocity in excess of 10^{-3} m/s. It is not unusual for the transformation toughened ceramics and corresponds to the minor nonlinearity of the load line and almost flat R-curve with a very steep rising part (Burns and Swain, 1986). After

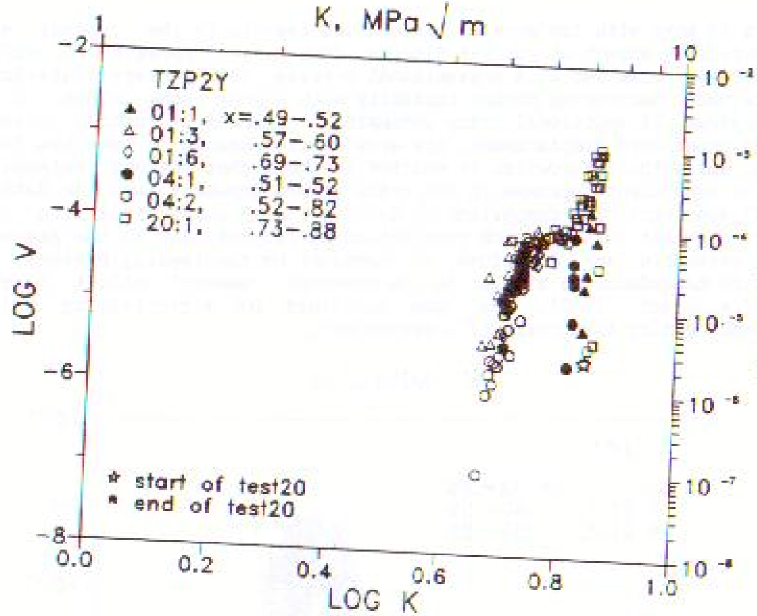

Fig. 4. Crack velocity vs stress intensity diagram for TZP2Y ceramics showing three-stage fracture kinetics behavior.

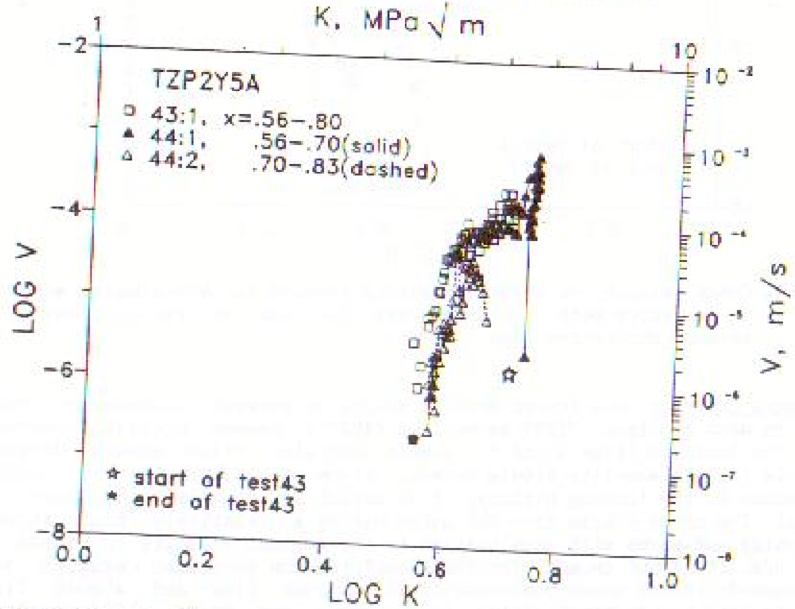

Fig. 5. Crack velocity vs stress intensity diagram for TZP2Y5A ceramics

allowing the crack to retard (TZP2Y-20 or TZP2Y5A-43) a considerable reduction in stress intensity follows, which corresponds to minor velocity changes, thus, the plateau-like region appears in the diagram (n = 4...8). Finally, after a certain "threshold" value of stress intensity is achieved, the crack turns into the arrest region, forming left-side extent of the steep slope in the diagram but in the low stress intensity range. Thus, the obtained V-K diagram will be referred to herein as having high-toughness steep, low-toughness steep, and plateau extents. It is obvious, that the diagram shows a well-defined similarity with the classic three-stage environmental slow crack growth diagram. However, all present experiments were conducted in the ambient laboratory environment (20...25 C, and relative humidity of 80...90%), hence, the appearance of middle plateau extent, typical of the extremely low humidity is unlikely to result from the environmental effect. It is expected to be caused by microstructure related phenomena. Li and Pabst (1980) found a similar feature in the slow crack growth behavior for Mg-PSZ ceramics with a relatively low content of tetragonal phase. However, in double torsion tests they could probably record only the middle and left parts of the diagram shown in Fig. 4 or 5, because the DT-measurements are carried out during the crack arrest stage. The abrupt change of the diagram slope was explained by the effective crack retardation, which takes place above the certain level of stress intensity. Another example of microstructure-induced effects reflected in the V-K diagram was observed by Troczinski and Nicholson (1991) for a glass-metallic composite, where the horizontal extent in the low stress intensity region was attributed to the growth and interconnection of microcracks at the notch tip. In our experiments, it is notable, that, for the second and following crack runs (see TZP2Y-01, 04 in Fig. 4, or TZP2Y5A-44 in Fig. 5), the starting stress intensity value was substantially lower as compared to that of the first run and does not exceed the limits of the low-toughness steep extent of the V-K diagram. This effect is believed to be similar to that observed by Li and Pabst, and may be explained as a consequence of stress-induced phase transformations. During the initial loading of the notched specimen, the transformation zone develops, that enduces the compression stress giving rise to the starting value of K. After that, the following decrease in the stress intensity is not accompanied by the equivalent crack velocity reduction as is dictated by the high-toughness steep extent of the diagram, and the crack rapidly overcomes the compression zone. When the crack growth run is repeated after full unloading, there is no more hindering influence of the starting compression zone, and the observed slow crack growth seems to occur without transformation toughening effects in the low region of the stress intensity variation. Transition from low-toughness steep extent of the V-K diagram to the plateau region (referred to a qualitative increase of crack retardation due to transformation; Li and Pabst, 1980) was never observed in anyone of subsequent runs, although the crack velocity did not exceed the upper boundary of the low-toughness extent. In contrast to the microcrack-induced behavior of alumina ceramics, in TZP ceramics an evident loss of high initial toughness is observed during both the subsequent monotonic crack extension with a decreasing stress intensity, and repeated successive crack runs under subsequent loading after initial full unloading. Hence, the probability is retained to initiate the slow crack growth inside the low toughness region, after the specimen or structural element is subjected to an overload. This in turn may be critical in any situation concerned with repeated loading, e.g., cyclic fatigue crack extension (Grathwohl and Liu, 1991).

CONCLUSIONS

Controlled testing of alumina ceramics shows an ambiguous slow crack growth diagram in confirmation of the "memory" effect attributed to the irreversible microcracking around the crack tip. In the test with successive crack runs in the same specimen crack resistance increases gradually in the crack acceleration extents with the slow crack growth exponent remaining almost unchanged. Respective crack retardation extents appear to be progressively shifted to higher stress intensities depending on the previous crack increment with a proportional increase in the crack growth exponent. For the transformation toughened zirconia of TZP2Y and TZP2Y5A grades the ambiguities in slow crack growth behavior are contradictory to those of microcracking in alumina. During crack acceleration from the starting notch, a relatively high level of crack resistance is demonstrated, but during subsequent retardation the crack missed the initial high level of toughness, and all subsequent extensions of the same crack show relatively low toughness values. Thus, the obvious "toughening relief" is observed. A decrease in stress intensity at the tip of retarding crack took place with minor variation in velocity, and characteristic plateau region appeared on the V-K diagram. The observed behavior (both for TZP2Y, and TZP2Y5A) is indicative of possible weak resistance to slow crack growth in some kinds of "tough" ceramics, which may be susceptible to low stress intensity cracking after surviving an overload, despite the high initial crack growth resistrance demonstrated in the R-curve test. Therefore, inequilibrium fracture behavior in fine-grained transformation toughened TZP-ceramics implies the limitations of R-curve concept application in determination of fracture resistance.

REFERENCES

1. V.G.Borovik, (1985). Strength of Mater., March, 1057-1061.
2. V.G.Borovik, S.P.Kovalev, and V.M.Chushko,(1990). Mechanics and Physics of Fracture in Brittle Materials (in Russ.), 70-74. Institute for Problems of Materials Science, Kiev.
3. S.J.Burns and M.V.Swain, (1986). J.Am.Ceram.Soc., 69, 226-30.
4. R.J.Fields, E.R.Fuller, Jr., T.J.Chuang, L.Chuck, and K.Kobayashi, (1983). Fracture Mechanics of Ceramics, 6, 463-73. Plenum.
5. S.W.Freiman, (1983). Fracture Mechanics of Ceramics, 6, 27-45. Plenum.
6. G.Grathwohl and T.Liu, (1991). J.Am.Ceram.Soc., 74, 318-25.
7. H.W.Hennicke, R.Görke, and W.Plentz, (1984). Science of Ceramics, 12, 599-606. Ceramurgia.
8. Y.H.Jung, K.R.Narendranath, P.S.Godavarti, and K.L.Murty, (1988). Eng. Fract. Mech., 29, 1-18.
9. F.W.Kleinlein and H.Hübner, (1977). Fracture'77, 3, 883-91. Pergamon.
10. R.Knehans and R.Steinbrech, (1982).J.Mater.Sci.Lett., 1, 327-29.
11. Li-Shing Li and R.F.Pabst, (1980). J.Mater.Sci., 15, 2861-66.
12. D.Munz, (1983). Fracture Mechanics of Ceramics, 6, 1-26. Plenum.
13. R.Pabst, (1975). Z. Werkstofftechnik, 6, 17-29.
14. J.E.Srawley, (1976). Int.J.Fract., 12, 475-76.
15. R.Steinbrech, R.Knehans, and W.Schaarwächter, (1983). J.Mater.Sci., 18, 265-70.
16. R.Steinbrech, H.Blanke, R.Knehans, and W.Schaarwächter, (1984). Science of Ceramics, 12, 655-60. Ceramurgia.
17. T.B.Troczynski and P.S.Nicholson, (1991). J.Am.Ceram.Soc., 74, 1803-06.
18. J.Wilde, W.Groll, and F.W.Kleinlein, (1985). J.Mater.Sci., 20, 4069-74.